Subsurface microscopy of interconnect layers of an integrated circuit

F. Hakan Köklü and M. Selim Ünlü*

Department of Electrical and Computer Engineering and the Photonics Center, Boston University, 8 Saint Mary's Street, Boston, Massachusetts 02215, USA
**Corresponding author: selim@bu.edu*

Received October 22, 2009; accepted November 22, 2009;
posted December 17, 2009 (Doc. ID 118907); published January 13, 2010

We apply the NA-increasing lens technique to confocal and wide-field backside microscopy of integrated circuits. We demonstrate 325 nm ($\lambda_0/4$) lateral spatial resolution while imaging metal structures located inside the interconnect layer of an integrated circuit. Vectorial field calculations are presented justifying our findings. © 2010 Optical Society of America

OCIS codes: 120.4630, 180.1790, 260.2110, 260.5430.

High-resolution far-field imaging necessitates the use of high-NA optical systems. Solid immersion lens (SIL) microscopy provides diffraction-limited imaging with high NA, taking advantage of the large refractive index of the immersion medium as well as the increased excitation and collection angles [1]. NA-increasing lens (NAIL) microscopy has been developed as an application of the SIL technique to subsurface imaging of integrated circuits (ICs) [2]. A Si NAIL placed on the backside of a polished silicon substrate effectively transforms the NAIL and the planar sample into an integrated SIL. This microscopy technique allows for high-resolution backside imaging through the substrate of an IC, as is often necessary because of opaque interconnect metal layers hindering frontside optical microscopy. Substrate and NAIL dimensions can be optimized for spherical aberration-free operation in central or aplanatic configurations [3]. The NAIL technique has been employed to enhance the imaging performance in wide-field and confocal imaging systems [2,4–6] as well as optical-beam-induced current imaging techniques [7].

The imaging studies to date have focused on the transistor layer that is fabricated within the surface layer of the silicon substrate. In this case, silicon with its high refractive index acts as the immersion medium enhancing the resolution. On the other hand, the proximity of a dielectric interface is a cause of image deformation. The effect of the dielectric interface in SIL imaging has been studied theoretically and experimentally [8,9]. There have been further efforts to isolate the optical signal coming from the transistor layer, from the optical signal coming from the interconnect layers by limiting the excitation to only high-incidence-angle light through the use of an annular aperture [10]. However, to our best knowledge, there has not been any study about the limits of subsurface imaging of the interconnect layer itself. Although most of the critical electrical components are located in the transistor layer, miniaturization of ICs made the first few metal interconnect layers extremely important for electrical performance [11]. Short-range effects such as capacitive coupling are crucial design and analysis considerations for the industry. Therefore, the ability to image the interconnect layers is invaluable for effective failure analysis. Unlike the transistor layer, interconnect layers of an IC are surrounded by the insulating dielectric, reducing the medium refractive index from ~3.5 in Si to ~1.5 in SiO_2 presenting additional challenges for imaging beyond the earlier experimental and theoretical studies. In this Letter, we study the limits of lateral spatial resolution for the interconnect layers of an IC in both confocal and widefield imaging schemes. In accordance with earlier studies, we quantify the effect that linearly polarized illumination has in confocal imaging [6,12]. We demonstrate a lateral spatial resolution of 325 nm ($\lambda_0/4$), in agreement with the values calculated theoretically.

The experimental setup is depicted in Fig. 1. The confocal microscopy part is a reflection-mode fiber optical scanning microscope operated at $\lambda_0 = 1.3$ μm, whereas the wide-field part uses LED illumination centered at 1.2 μm. The wide-field part has a larger field of view, making on-chip-navigation easier, and has the ability to acquire high-magnification images by using a zoom module. A sliding mirror enables us to rapidly switch between confocal and wide-field imaging modalities. When the sliding mirror is out, in

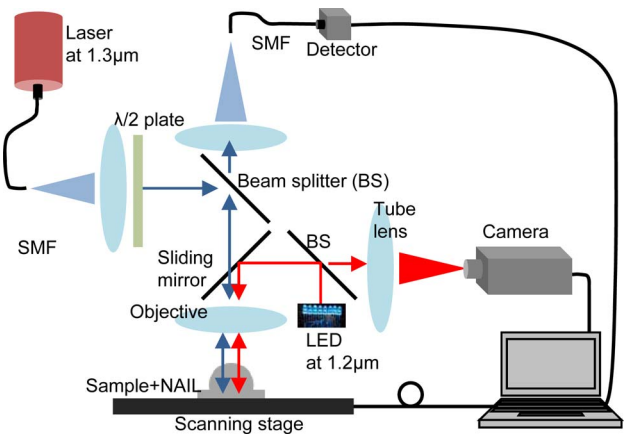

Fig. 1. (Color online) Experimental setup. A sliding mirror provides switching between confocal and widefield microscopes. A half-wave plate is used to rotate the polarization of the illumination in confocal imaging. SMF, single-mode fiber.

confocal imaging, incoming illumination from the side and detected signal going to the top are separated with a beam splitter. A full confocal image is acquired by the use of a piezoelectric stage that raster scans the sample with a NAIL. When the sliding mirror is in, the sample is illuminated with a LED array, and the image is captured by an InGaAs CCD camera. The focusing objective with an NA of 0.26 is suitable for NAIL microscopy.

The NAIL used in this work is an undoped Si hemisphere with radius $R=1.61$ mm. The optimum substrate thickness (X) for aplanatic imaging with this NAIL is $X=R/n$ equal to 460 and 457 μm, respectively for $\lambda_0=1.3$ μm and $\lambda_0=1.2$ μm, where n is the refractive index at the operating wavelengths [3]. The sample is a custom IC with four metal and two polysilicon layers fabricated at Austriamicrosystems by a 0.35 μm process. The substrate thickness was reduced to 458 ± 2 μm for aplanatic imaging in both operating wavelengths.

The sample IC has passive parallel lines on metal 1 (m1), metal 2 (m2), metal 3 (m3), and metal 4 (m4) layers for calibration. The linewidths and spacings are 0.6, 0.8, 1, and 2 μm for m2, m3, and m4 layers, whereas there is an additional set of 0.5 μm lines on the m1 layer as allowed by the design rules. We are presenting the images of the lines with 0.5 μm width and spacing located on the m1 layer and 0.6 μm width and spacing located on the m4 layer for two different polarization directions that are parallel and perpendicular to the lines, respectively, in Figs. 2(a) and 2(b). In Fig. 2(c), images taken with the widefield microscope are presented. In confocal images, the lines that are parallel to the polarization direction have sharper edges as expected from the theory. Although the image quality is not as good as in confocal imaging, the lines are resolved in wide-field images as well. The low signal-to-noise ratio prevents us from acquiring higher-magnification images in wide-field microscopy. One way to improve the widefield images can be by using low-NA optics to reduce the light that is reflected and scattered at the $Si-SiO_2$ interface. The incoming optical field components with NAs bigger than 1.5 are reflected at the $Si-SiO_2$ interface and never make it to the interconnect layers. In confocal imaging, these reflections do not contribute to the detected signal, since they are well outside the confocal volume. However, in widefield imaging these reflections and the scattered light cause a pronounced background, reducing the contrast of the acquired images. Employing a low-NA objective [13] or mounting an iris at the back aperture of the objective is expected to improve the visibility of widefield images.

We used the Houston criterion to quantify the resolution for different layers, polarization states, and imaging modalities. We imaged the lines with 1 μm width and spacing and recorded the edge responses. Line spread functions (LSFs) have been extracted from the edge responses to estimate the resolution, which is defined as the FWHM of the LSF for the Houston criterion. Figure 3 illustrates sample edge responses taken from the confocal images and the

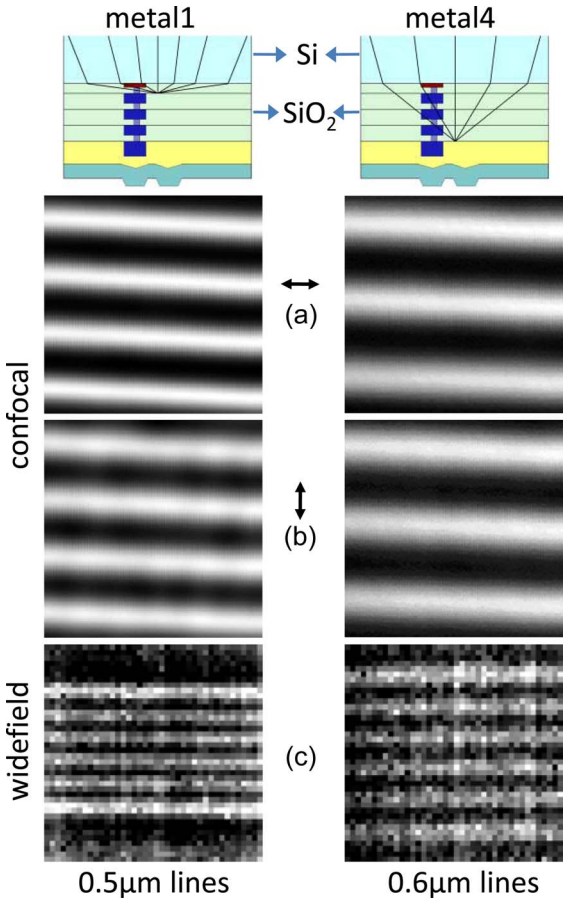

Fig. 2. (Color online) (a) Confocal image of m1 lines under horizontal polarization on the left and m4 lines on the right. (b) Same as (a) with vertical polarization. (c) Widefield image of m1 lines on the left and m4 lines on the right.

corresponding LSFs for m1 and m4 layers for two polarization directions. As indicated in Fig. 3, measured resolutions as are 325 and 450 nm for m1 lines where the edge responses were recorded in the direction perpendicular and parallel to the polarization direction of the illumination, respectively. Corresponding resolutions for the m4 layer have been measured as 340 and 460 nm. Since the images and the resolution data for the m2 and m3 layers are very similar, they are not included. Although the resolutions for the m1 layer seem to be better than for the m4 layer, measurements do not show a conclusive enhancement

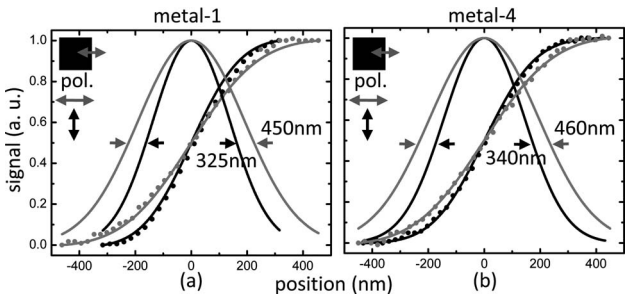

Fig. 3. Edge response data and corresponding LSFs for confocal imaging of m1 and m4 layers. Gray curves correspond to the line cut direction parallel to the polarization direction, whereas black curves correspond to the perpendicular direction.

trend from the m4 to the m1 layer. The edge responses for wide-field microscopy are averaged over 50 line cuts to have an accurate measurement, and the resolution is estimated to be ~450 nm with a standard deviation of 100 nm for all layers. Relatively noisy wide-field image data prevents us from including a representative edge response that would reflect this calculation.

We have calculated the focal field distributions, using angular spectrum representation [14] for the light that is focused at 0.65 and 3.65 μm beyond the interface as specified by the manufacturer specifications for the depth of m1 and m4 layers, respectively. Angular spectrum representation enables us to take into account the polarization of the incoming light under high-NA conditions as well as the polarization-dependent refraction and reflection at the dielectric interface. The focused fields at the depths of m1 and m4 are shown in Fig. 4. The field distributions in the $x-z$ and $y-z$ planes are shown separately to exhibit the effect of polarization when the incoming light is polarized in the x direction. As is evident from the calculations, there is no significant change in lateral spot size from m1 depth to m4 depth. However, spherical aberrations due to the refraction at the interface lengthen the extent of the focal spot in the z direction. Confocal LSFs were computed from the field calculations for comparison with the experimental results. For the m1 layer, calculated resolution values are 310 and 520 nm when line cut directions are perpendicular and parallel to the polarization direction, respectively. The fact that the experimental value in the direction parallel to polarization is better than the theoretical value can be due to imperfect polarization. For the m4 layer, calculated results are 360 and 450 nm when line cut directions are perpendicular and parallel to the polarization direction, respectively, virtually identical to the experimental values.

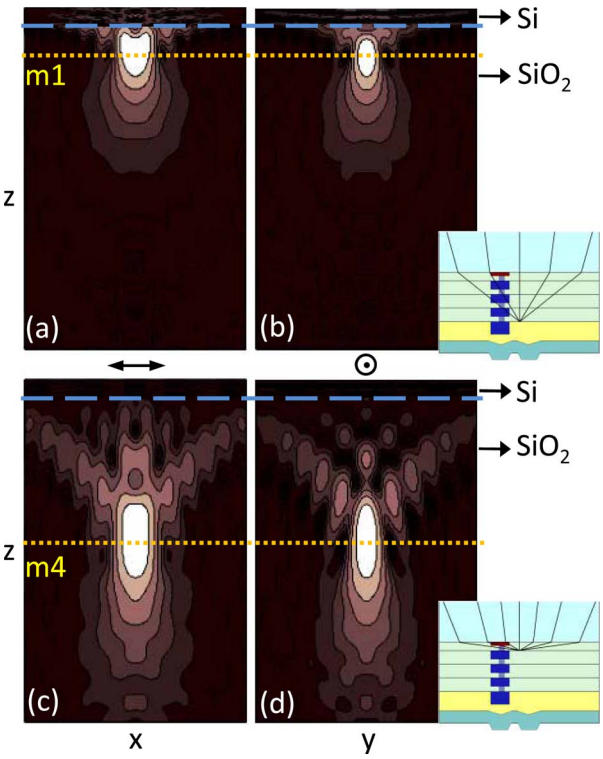

Fig. 4. (Color online) Focal field distributions calculated with angular spectrum representation for the light that is focused at (a) 0.65 μm and (b) 3.65 μm beyond the interface for the depth of m1 and m4 layers, respectively. Incoming light is polarized in the x direction as indicated.

In this study, we conducted the first experimental demonstration of lateral spatial resolution characterization in subsurface backside imaging of interconnect layers of an integrated circuit. We have shown a lateral spatial resolution of 325 nm ($\lambda_0/4$) for the first metal layer in confocal imaging. We have also demonstrated 450 nm resolution with the wide-field imaging system. These results cannot challenge the typical lateral resolutions of 200 nm attained when imaging the transistor layer because of the much smaller medium refractive index. However, the results presented here show that the first few interconnect layers can be imaged without considerable spherical aberration caused by the dielectric interface. The ability to resolve interconnect layers with this resolution is of great significance for interpreting short-range effects and electrical performance in modern integrated circuits.

The authors wish to thank Justin I. Quesnel for sample fabrication. This work was supported by Air Force Office of Scientific Research under grant MURI F-49620-03-1-0379.

References and Notes

1. S. M. Mansfield and G. S. Kino, Appl. Phys. Lett. **57**, 2615 (1990).
2. S. B. Ippolito, B. B. Goldberg, and M. S. Ünlü, Appl. Phys. Lett. **78**, 4071 (2001).
3. S. B. Ippolito, B. B. Goldberg, and M. S. Ünlü, J. Appl. Phys. **97**, 053105 (2005).
4. S. B. Ippolito, S. A. Thorne, M. G. Eraslan, B. B. Goldberg, M. S. Ünlü, and Y. Leblebici, Appl. Phys. Lett. **84**, 4529 (2004).
5. F. H. Koklu, J. I. Quesnel, A. N. Vamivakas, S. B. Ippolito, B. B. Goldberg, and M. S. Ünlü, Opt. Express **16**, 9501 (2008).
6. F. H. Koklu, S. B. Ippolito, B. B. Goldberg, and M. S. Ünlü, Opt. Lett. **34**, 1261 (2009).
7. E. Ramsay, K. A. Serrels, M. J. Thomson, A. J. Waddie, M. R. Taghizadeh, R. J. Warburton, and D. T. Reid, Appl. Phys. Lett. **90**, 131101 (2007).
8. K. Karrai, L. Xaver, and L. Novotny, Appl. Phys. Lett. **77**, 3459 (2000).
9. L. Novotny, R. D. Grober, and K. Karrai, Opt. Lett. **26**, 789 (2001).
10. S. B. Ippolito, P. Song, D. L. Miles, and J. D. Sylvestri, Appl. Phys. Lett. **92**, 101109 (2008).
11. ITRS, *International Technology Roadmap for Semiconductors* (2007).
12. K. A. Serrels, E. Ramsay, R. J. Warburton, and D. T. Reid, Nat. Photonics **2**, 311 (2008).
13. The optimum NA of the objective should be selected as $NA=1.5/n^2=0.12$ for this case [3].
14. B. Richards and E. Wolf, Proc. R. Soc. London Ser. A **253**, 358 (1959).